

## IMECE2006-14740

## CASCADE CONTROL WITH FRICTION COMPENSATION BASED ON ARTIFICIAL NEURAL NETWORK FOR A HYDRAULIC ACTUATOR

**Cláudio Luís d' Elia Machado**

Pelotas Federal Centre for  
Technological Education  
Pelotas,RS, 96015-360  
Brazil  
claudiomachado@cefetrs.tche.br

**Raul Guenther**

**Victor Juliano De Negri**  
Mechanical Engineering Department  
Federal University of Santa Catarina  
Florianópolis,SC, 88040-900  
Brazil  
guenther@emc.ufsc.br  
victor@emc.ufsc.br

**Sebastião Cícero Pinheiro Gomes**

Federal University of Rio Grande  
Rio Grande,RS, 96201-900  
Brazil  
dmtscpg@furg.br

### ABSTRACT

This paper addresses the friction compensation in hydraulic actuators using an artificial neural network combined with a suitable control technique. The proposed neural network is trained off-line and allows calculate an estimative of the friction force on-line very quickly based on the hydraulic force and on the cylinder velocity. The estimated friction force is introduced directly in the force line of the system using a cascade controller, in which the hydraulic actuator is interpreted as two interconnected subsystems: a mechanical one driven by a hydraulic one. The convergence properties of the closed loop system are established using the Lyapunov method. Experimental results validate the main theoretical results of the proposed strategy.

### NOMENCLATURE

$A$  Cylinder piston area [ $m^2$ ]  
 $c_d$  Dead-zone compensation parameter [ $V$ ]  
 $c_e$  Dead-zone compensation parameter [ $V$ ]  
 $d$  Input disturbance [ $N$ ]  
 $e$  Neural network input  
 $\tilde{\mathbf{F}}$  Force vector  
 $\bar{\mathbf{F}}$  Upper bound force vector  
 $F_A$  Friction force [ $N$ ]

$\hat{F}_A$  Estimated friction force [ $N$ ]  
 $\tilde{F}_A$  Estimated friction force error [ $N$ ]  
 $F_{Ac}$  Friction force training patterns [ $N$ ]  
 $F_L$  External force [ $N$ ]  
 $f$  Nonlinear function  
 $g$  Nonlinear function  
 $h$  Neural network activation function  
 $K_D$  Mechanical subsystem control law gain [ $N.s.m^{-1}$ ]  
 $K_P$  Hydraulic subsystem control law gain [ $s^{-1}$ ]  
 $K_s$  Valve flow coefficient [ $m^4.V^{-1}.s^{-1}.N^{-1/2}$ ]  
 $l_c$  Dead-zone compensation parameter [ $V$ ]  
 $M$  System's total mass [ $kg$ ]  
 $p_a$  Pressure in the line  $a$  [ $Pa$ ]  
 $p_b$  Pressure in the line  $b$  [ $Pa$ ]  
 $p_s$  Supply pressure [ $Pa$ ]  
 $p_\Delta$  Pressure difference [ $Pa$ ]  
 $\tilde{p}_\Delta$  Pressure difference tracking error [ $Pa$ ]  
 $p_{\Delta d}$  Desired pressure difference [ $Pa$ ]  
 $R$  Positive constant  
 $s$  Velocity trajectory tracking error [ $m.s^{-1}$ ]  
 $t$  Time [ $s$ ]  
 $t_s$  Sample period [ $s$ ]  
 $u$  Valve control input [ $V$ ]  
 $u_c$  Controller signal [ $V$ ]  
 $V$  Lyapunov function  
 $v$  Total volume [ $m^3$ ]

$v_a$	Oil volume in the lines $a$ [ $m^3$ ]
$v_b$	Oil volume in the lines $b$ [ $m^3$ ]
$w$	Neural network weight
$y$	Position trajectory [ $m$ ]
$\tilde{y}$	Position trajectory tracking error [ $m$ ]
$y_d$	Desired position trajectory [ $m$ ]
$\dot{y}_r$	Reference velocity [ $m.s^{-1}$ ]
$\beta$	Oil bulk modulus [ $Pa$ ]
$\lambda$	Mechanical subsystem control law gains [ $s^{-1}$ ]
$\lambda_{min}$	Minimum eigenvalue
$\rho$	Error vector

## INTRODUCTION

Hydraulic actuators provide high force, stiffness and durability suitable to various applications, and there is a growing demand for such actuators to operate with improved precision and repeatability. Unfortunately, these actuators present some undesirable characteristics, namely, lightly damped dynamics and highly non-linear behavior introduced by both, pressure dynamics and friction, among others.

In a typical hydraulic actuator, the movement of the piston, and hydraulic fluid are subject to friction. The friction is generated by the contact between both the rod and the seal, and the piston seal and the cylinder, and the viscous effects of the hydraulic fluid. This friction affects the controllability, accuracy, and repeatability of the actuator.

The lightly damped dynamics and the non-linear flow and friction dynamics complicate the controller design for high performance closed loop applications. The simple classical controllers cannot overcome the bandwidth limitation caused by the lightly damped open loop poles position. The use of a linear controller is limited by the non-linear behavior.

Due to these control difficulties, a combination of non-linear control techniques offers good theoretical and experimental results. One way to combine control techniques is to use the backstepping method. Another way to do it is based in interpreting the hydraulic actuator as two interconnected subsystems: a mechanical subsystem driven by a hydraulic one.

In this paper is chosen the second method in which the main idea is to promote a fast loop in the hydraulic subsystem in order to generate hydraulic forces that allow the mechanical subsystem to track the desired trajectory. This idea was formalized in [1,2] taking into account an error during the hydraulic subsystem trajectory tracking and by presenting a stability proof of the whole interconnected system. The resulting controller is referred as cascade controller. The experimental and theoretical results employing this controller have demonstrated that its closed loop performance overcomes the performance obtained with classical controllers, with respect to the lightly damped dynamics and to the non-linear pressure dynamics. In this paper is shown that the cascade controller allows compensate the friction dynamics in a

very simple and efficient way.

Friction is a complicated phenomenon that is still not fully understood [3]. Stick-slip friction is a nonlinear friction phenomenon and can be found in hydraulic actuators around the zero velocity range. Before motion starts, the surfaces are in the static friction regime. A force greater than the static friction is required to begin the movement. As the component starts to move, the friction suddenly decreases as it switches to the dynamic friction regime. This sudden change in friction results in a jerky actuator motion, making positional control and repeatability difficult [3–5].

Modeling this sudden switch is difficult and has been addressed by several researches. A review can be found in [3]. More recently a model based on the concept of a variable friction coefficient was proposed and applied to in [6], which well represents the stick-slip modes.

Generally the friction compensation consists in adding an estimated friction force to the force reference generated by the position controller. This kind of compensation assumes that the actuator has a fast and accurate force response. This is generally verified with electric actuators. Nevertheless, most servovalves, which are the control devices of the hydraulic actuators, do not provide a sufficient fast and efficient force response.

The approach presented in this paper allows to add the estimated friction force to the force reference of the mechanical subsystem of the cascade controller and to provide a sufficiently fast response in the hydraulic subsystem in order to compensate the friction.

The friction force is estimated off-line using a neural network which architecture is based on the model with the variable friction coefficient [6]. This neural network possesses a simple architecture and is easily implemented on-line.

The cascade controller with this friction compensation improves the tracking performance as predicted in the theoretical discussion presented in this paper and it is confirmed by the experimental results.

The paper is organized as follows. First is described the hydraulic actuator model and the cascade strategy. Next, the cascade controller with friction compensation is presented. In the sequence, the friction force estimation is described. Then is presented the cascade controller stability analysis, describe the experimental setup and discuss the experimental results. Finally is outlined some conclusions.

## HYDRAULIC ACTUATOR MATHEMATICAL MODEL

The hydraulic actuator considered in this paper is shown in Fig. 1. It consists of a double-rod cylinder controlled by a supercritical center four-way spool valve. In this modeling, it is considered that the hydraulic power unit delivers a constant supply pressure  $p_s$  irrespective of the oil flow rate.

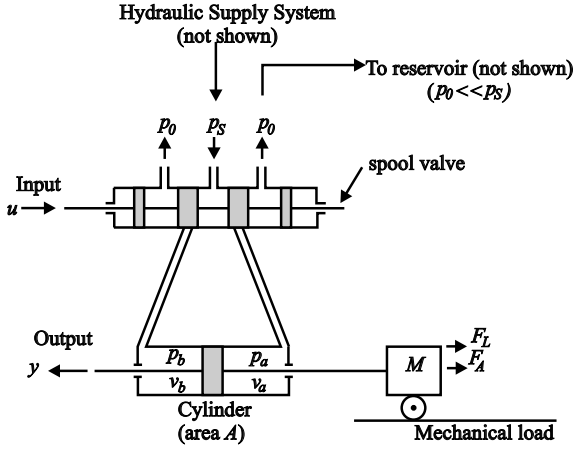


Figure 1. HYDRAULIC ACTUATOR

In Fig. 1,  $p_0$  is the return pressure,  $p_a$  is the pressure in the line  $a$ ,  $p_b$  is the pressure in the line  $b$ ,  $v_a$  is the oil volume in the lines  $a$ ,  $v_b$  is oil volume in the lines  $b$ ,  $A$  is the cylinder piston cross-sectional area,  $M$  represents the total mass of the system,  $F_A$  is the nonlinear friction,  $y$  is the actuator piston position,  $F_L$  represents an external force, and  $u$  is the control input.

When the valve dynamics is sufficiently fast and can be neglected, the hydraulic actuator can be represented by the following nonlinear equations [7]

$$M\ddot{y} + F_A = A p_\Delta - F_L \quad (1)$$

$$\dot{p}_\Delta = A f(y)\dot{y} + K_s g(u, p_\Delta) u \quad (2)$$

where,  $p_\Delta = p_a - p_b$  is the pressure difference between the chambers  $a$  and  $b$  of the cylinder and  $K_s$  is the valve flow coefficient. The nonlinear functions  $f(y)$  and  $g(u, p_\Delta)$  are given, respectively, by

$$f(y) = \frac{\beta v}{(0.5v^2) - A y^2} \quad (3)$$

$$g(u, p_\Delta) = \sqrt{p_s - \frac{u}{|u|} p_\Delta} \quad (4)$$

where  $\beta$  is the bulk modulus,  $v$  is the total volume of oil.

As it is observed, the valve model is represented by the second term of Eq. (2), assuming that exists a linear relation between the tension and the flow for a given pressure difference value. This represents adequately the tension versus flow curve presented in the valve catalog [8], non considering the valve

dead-zone. This model represents well the real system behavior since the dead-zone is compensated, as shown in the Experimental Setup section.

The model presented in this section will be used in the sequel.

## THE CASCADE STRATEGY

The hydraulic actuator can be interpreted as two interconnected subsystems: a mechanical subsystem driven by a hydraulic one. This interpretation is shown in Fig. 2 and can be physically explained as follows.

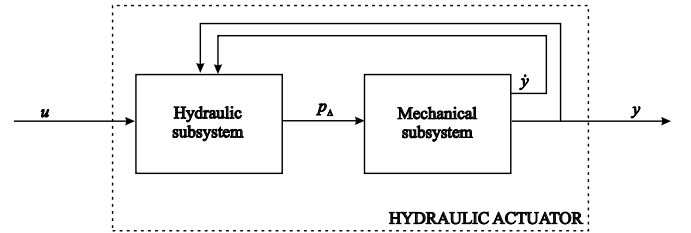


Figure 2. INTERCONNECTED SUBSYSTEMS

In the hydraulic actuator shown in Fig. 1, when the valve spool is moved in one direction, the pressure in one chamber starts to increase and the pressure in the other chamber starts to decrease. It creates a pressure difference  $p_\Delta$  between the chambers and generates a force on the cylinder piston. This force is applied to a mass-damper system (mechanical subsystem). Therefore, the mechanical subsystem is driven by a hydraulic one. On the other hand, the fluid dynamics in the chambers of the hydraulic subsystem is affected by the piston movement, and this shows the system interconnection.

This interpretation is used by several authors to develop controllers for hydraulic actuators [9–11]. The idea is to promote a fast loop in the hydraulic subsystem in order to generate a force in the hydraulic subsystem that allows the mechanical subsystem to track the desired trajectory. In [1] this idea was formalized taking into account an error during the hydraulic subsystem trajectory tracking. Also, the stability proof for the whole system and the resulting strategy is presented in this paper.

The control objective is that  $y(t)$  tracks a desired trajectory  $y_d(t)$  as close as possible. To achieve this end, let

$$\tilde{p}_\Delta = p_\Delta - p_{\Delta d} \quad (5)$$

be the pressure difference tracking error, where  $p_{\Delta d}$  is the desired pressure difference so that the control goal is reached. Substitu-

ting Eq. (5) into Eq. (1) gives

$$M\ddot{y} + F_A = Ap_{\Delta d} + d(t) \quad (6)$$

where  $d(t) = A\tilde{p}_{\Delta} - F_L$  is an input disturbance.

The system described by Eq. (6) and (2) is in the cascade form. Equation (6) can be interpreted as a second order mechanical subsystem driven by a desired force  $Ap_{\Delta d}$  and subjected to an input disturbance  $d(t)$ . Equation (2) represent the hydraulic subsystem.

The design of the cascade controller for the system in Eq. (6) and (2) can be summarised as:

- (i) Compute a control law to the mechanical subsystem Eq. (6) such that the cylinder displacement  $y$  achieves a desired position trajectory  $y_d(t)$  taking into account the presence of the disturbance  $d(t)$ . With this desired force  $Ap_{\Delta d}$  one can quantify the desired pressure difference;
- (ii) Compute a control law  $u$  such that  $p_{\Delta}$  tracks  $p_{\Delta d}$  defined above as close as possible.

## CASCADE CONTROLLER WITH FRICTION COMPENSATION

Using the cascade control strategy it is possible to introduce the friction compensation at the force level, i.e. at the input of the mechanical subsystem. So, the estimated friction force  $\hat{F}_A$  is considered as an additional input in this subsystem, as is shown in Fig. 3.

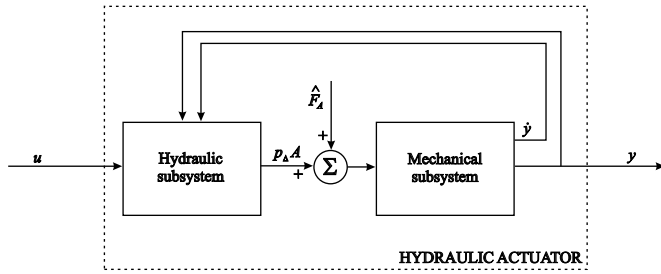


Figure 3. FRICTION COMPENSATION IN THE CASCADE CONTROL

The desired pressure difference required in order to the position  $y$  track  $y_d$  is calculated by using a Slotine and Li control law [12] given by

$$p_{\Delta d} = \frac{1}{A} \left( M\dot{y}_r + \hat{F}_A - K_D s \right) \quad (7)$$

where

$$\dot{y}_r = \dot{y}_d - \lambda \tilde{y}, \quad \tilde{y} = y - y_d, \quad s = \dot{y} - \dot{y}_r = \dot{\tilde{y}} + \lambda \tilde{y} \quad (8)$$

where  $\dot{y}_r$  is the reference velocity,  $s$  is a measure of the trajectory tracking error,  $K_D > 0$  and  $\lambda > 0$  are the mechanical subsystem control law gains and  $\tilde{y}$  is the position trajectory tracking error.

The hydraulic subsystem control law contains the inverse of the functions  $f(y)$  and  $g(u, p_{\Delta})$ , defined in Eq. (3) and (4), respectively, and is given by

$$u = \frac{1}{K_s g(u, p_{\Delta})} \left[ \frac{1}{f(y)} (\dot{p}_{\Delta d} - K_P \tilde{p}_{\Delta}) + A\dot{y} \right] \quad (9)$$

where  $K_P$  is the proportional gain, and  $\dot{p}_{\Delta d}$  is the time derivative of the desired pressure difference given in Eq. (7).

Consider that the system parameters are exactly known and the external force  $F_L$  is null. Combining Eq. (6) and Eq. (7) and using (8), the Eq. (6) can be rewritten by

$$M\dot{s} + K_D s = A\tilde{p}_{\Delta} - \tilde{F}_A \quad (10)$$

where  $\tilde{F}_A = F_A - \hat{F}_A$  is the error in the estimated friction force.

Substituting the control law Eq. (9) in Eq. (2) and in the time derivative of Eq.(5), taken into account again that the system parameters are exactly known, it results

$$\dot{\tilde{p}}_{\Delta} = -K_P \tilde{p}_{\Delta} \quad (11)$$

*Remark:* To deal with the system parameter uncertainties, an algorithm named VS-ACC combining an adaptive control law for the mechanical subsystem and a variable structure control law for the hydraulic subsystem was proposed in [7].

## FRICTION FORCE ESTIMATION

In this paper the friction force in the hydraulic cylinder is estimated off-line using a neural network (NN).

The NN architecture proposed to learn the friction force is a multi-layer fully connected feed-forward network [13], using back propagation with momentum [14] as the training rule. The input layer has two neurons corresponding to the hydraulic force and the cylinder velocity, respectively. The output layer is composed by one neuron (friction force). The hidden layer has only four neurons, as it is shown in Fig. 4.

The friction model based on the concept of a variable viscous friction coefficient introduced by [15], which allows to represent well the stick-slip modes, motivated the conception of this architecture.

The hidden layer was defined after testing several feed-forward network configurations in order to identify a configuration able to learn and to reproduce the training patterns with a minimum of neurons as done in [15].

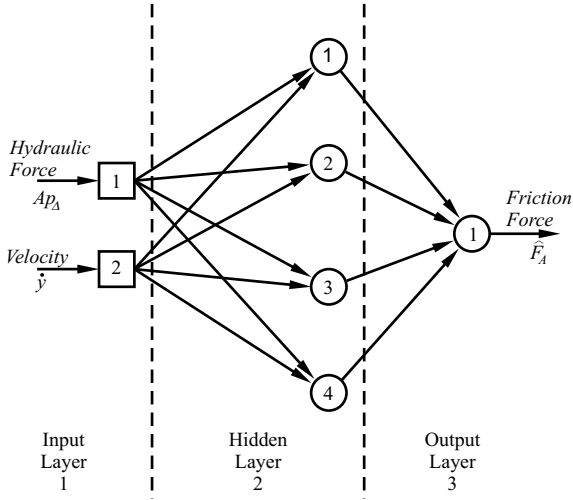


Figure 4. NEURAL NETWORK ARCHITECTURE

The NN shown in Fig. 4 can be represented by

$$\hat{F}_A = h_1 \left( \sum_{j=1}^4 w_{j1}^o h_j \left( \sum_{i=1}^2 w_{ji}^h e_i + w_{j3}^h \right) + w_5^o \right) \quad (12)$$

where  $\hat{F}_A$  is the estimated friction force,  $h$  is the activation function,  $w^h$  and  $w^o$  are the weights of the hidden and output layers, respectively,  $e_1 = Ap_{\Delta}$  is the hydraulic force and  $e_2 = \dot{y}$  is the velocity. Is used the hyperbolic tangent as function activation.

The training consists in adjusting the values of the weights of each node using the backpropagation with momentum method [14] with the input and output patterns established experimentally.

The hydraulic force training patterns are calculated using the measured chamber pressures  $[A(p_a - p_b)]$  and are shown in Fig. 5. The velocity training patterns are obtained by a numeric derivative process of the measured cylinder position and are shown in Fig. 6.

The output patterns corresponding to the friction force are calculated using the chambers measured pressures and the acceleration  $\ddot{y}$  obtained by the numeric derivative of the velocity, i.e.

$$F_{Ac} = (p_a - p_b)A - M\ddot{y} \quad (13)$$

This friction force training patterns ( $F_{Ac}$ ) are presented in Fig. 7.

The training begins with an initial set of weights that are adjusted according the network response to the input patterns which is supervised by the output patterns (friction force).

The training is interrupted when the total output errors (relationship between the sum of the errors by the number of samples)

is less than 1 % or with a total of 10000 iterations. The NN response is shown in Fig. 8 and the obtained weights are shown in the Table 1.

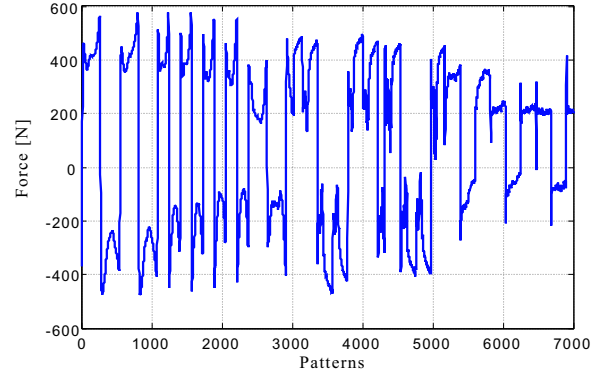


Figure 5. HYDRAULIC FORCE TRAINING PATTERNS

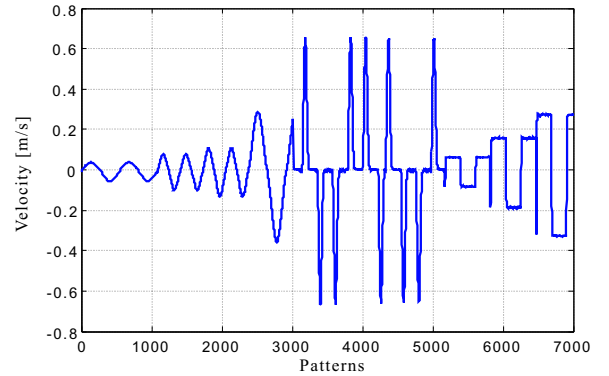


Figure 6. VELOCITY TRAINING PATTERNS

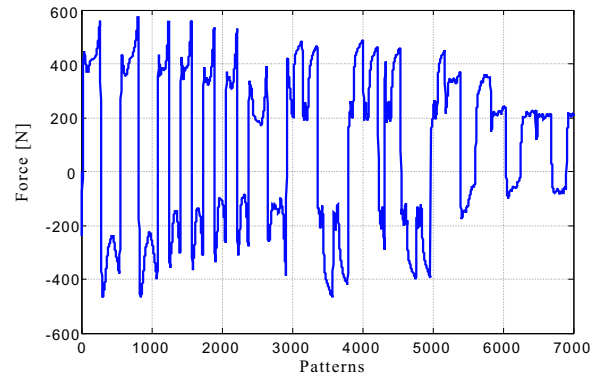


Figure 7. FRICTION FORCE TRAINING PATTERNS

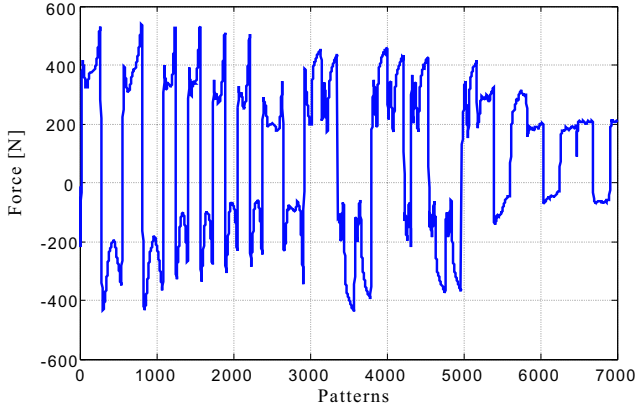


Figure 8. NEURAL NETWORK RESPONSE

Table 1. TRAINING RESULTS

$w_{11}^h = [2.090 \quad 0.6337 \quad 2.326]^T$
$w_{21}^h = [-0.038 \quad 3.712 \quad -0.067]^T$
$w_{31}^h = [-3.085 \quad -0.942 \quad 3.561]^T$
$w_{41}^h = [0.675 \quad 3.048 \quad -0.198]^T$
$w_{12}^o = [1.093 \quad -0.872 \quad -1.812 \quad 1.099 \quad 0.872]^T$

It should be outlined that the proposed neural network architecture is simple (see Fig. 4) and it is very easy to be implemented on-line (Eq. (12)).

## THE CASCADE CONTROLLER STABILITY ANALYSIS

The cascade controller is obtained by combining the mechanical subsystem tracking control law (Eq.(7)), the estimated friction force given in Eq.(12), and the control signal designed to achieve the hydraulic subsystem pressure tracking given by Eq. (9).

Consider the closed loop system given by  $\Omega = \{ (6), (2), (7), (9) \}$ . In an ideal case, in which all the system parameters are known, the tracking error convergence properties are presented below.

*Theorem:* When all the system parameters are known, the closed loop  $\Omega$  is globally stable and the tracking errors  $\tilde{y}(t)$  and  $\tilde{y}'(t)$  converge to a residual set  $\mathbf{R}$  as  $t \rightarrow \infty$ . The set  $\mathbf{R}$  depends on the friction compensation efficiency.

*Proof:* Consider the nonnegative function

$$2V = Ms^2 + R\tilde{y}^2 + \tilde{p}_\Delta^2 = \rho^T \mathbf{N}_1 \rho \geq 0 \quad (14)$$

where  $R$  is a positive constant given by  $R = 2\lambda K_D$  and the matrix

$\mathbf{N}_1$  is given by

$$\mathbf{N}_1 = \begin{bmatrix} \lambda^2 M + R & \lambda M & 0 \\ \lambda M & M & 0 \\ 0 & 0 & 1 \end{bmatrix} \quad (15)$$

and the error vector is defined as  $\rho = [\tilde{y} \quad \tilde{y}' \quad \tilde{p}_\Delta]^T$ . The time derivative of  $V$  is given by

$$\dot{V} = -K_D s^2 + R\tilde{y}\tilde{y}' + A\tilde{p}_\Delta s - \tilde{F}_{A,s} - K_P \tilde{p}_\Delta^2 \quad (16)$$

Expression (16) can be written as

$$\dot{V} = -\rho^T \mathbf{N}_2 \rho - \rho^T \tilde{\mathbf{F}} \quad (17)$$

where the matrix  $\mathbf{N}_2$  is

$$\mathbf{N}_2 = \begin{bmatrix} \lambda^2 K_D & 0 & -\frac{1}{2}\lambda A \\ 0 & K_D & -\frac{1}{2}A \\ -\frac{1}{2}\lambda A & -\frac{1}{2}A & K_P \end{bmatrix} \quad (18)$$

and the force vector  $\tilde{\mathbf{F}}$  is defined as

$$\tilde{\mathbf{F}} = [-\tilde{F}_A \lambda \quad -\tilde{F}_A \quad 0]^T \quad (19)$$

Employing the matrix theory it could be shown that the matrix  $\mathbf{N}_2$  is positive definite if the gains are related by the condition

$$K_D K_P > 0.5A^2 \quad (20)$$

Using the theorem of Rayleigh-Ritz, the Eq. (17) can be written

$$\dot{V} = -\lambda_{\min}(\mathbf{N}_2) \|\rho\|^2 - \|\rho\| \tilde{\mathbf{F}} \quad (21)$$

where  $\|\rho\|$  is the error vector norm,  $\lambda_{\min}(\mathbf{N}_2)$  is the minimum eigenvalue of the matrix  $\mathbf{N}_2$  and  $\tilde{\mathbf{F}}$  is the norm of an upper bound of the vector defined in Eq. (19).

From Eq. (22) is concluded that under condition (20) the time derivative  $\dot{V}$  is negative when

$$\|\rho\| > \frac{\tilde{\mathbf{F}}}{\lambda_{\min}(\mathbf{N}_2)} \quad (22)$$

Expressions (14) and (22) show that  $\|\rho\|$  tends to a residual set which depends on  $\bar{\mathbf{F}}$  and on  $\lambda_{min}(\mathbf{N}_2)$  as  $t \rightarrow \infty$ . Consequently, each error component tends to a residual set. So, the tracking errors  $\tilde{y}(t)$  and  $\tilde{\dot{y}}(t)$  tends to a residual set as  $t \rightarrow \infty$ .

## EXPERIMENTAL SETUP

The experimental implementation was performed on a test rig composed of a double-rod cylinder, a proportional valve NG6 [8] and its electronic card, a data acquisition and control board DS 1102 dSPACE, pressure transducers, thermocouple, position transducer, and a power and conditioning hydraulic unit. The experimental setup are shown in Figs. 9 and 10. The hardware for the control scheme is shown in Fig. 11.



Figure 9. EXPERIMENTAL SETUP

Considering the hydraulic actuator model presented, the system parameters are  $M = 20.66kg$ ,  $A = 7.6576 \times 10^{-4} m^2$ ,  $v = 9.5583 \times 10^{-4} m^3$ ,  $\beta = 9 \times 10^8 Pa$  and  $p_s = 10MPa$ .

From the valve catalog, is taken that the nominal flow rate is  $5.83 \times 10^{-4} m^3 \cdot s^{-1}$  ( $35L \cdot min^{-1}$ ) at a pressure differential of  $0.8MPa$ . In this practical application the input  $u$  is the electronic amplifier input and  $u$  can assume values between  $-10V$  and  $+10V$ , and  $K_s = 6.55 \times 10^{-8} m^4 V^{-1} s^{-1} N^{-1/2}$ .

In order to reduce the noise in the measured pressures and cylinder position, is used first order filters adjusted according to the transducers calibration curve. The used bandwidth is  $\omega_f = 80rad/s$ .

The valve is commanded by an electronic card with a circuit that reproduces a dead-zone inverse, which may be used to compensate the valve dead-zone. This electronic card also has an electrical dead-zone [16]. Therefore, even if the valve dead-zone could be compensated by the electronic card circuit, there would be a dead-zone in the relation between the electronic card input

voltage and the flow rate in the valve, caused by this electrical dead-zone. To overcome this problem, is used a dead-zone compensation placed between the control signal  $u$  generated by the control algorithm and the D/A converters (voltage applied to the electronic card).

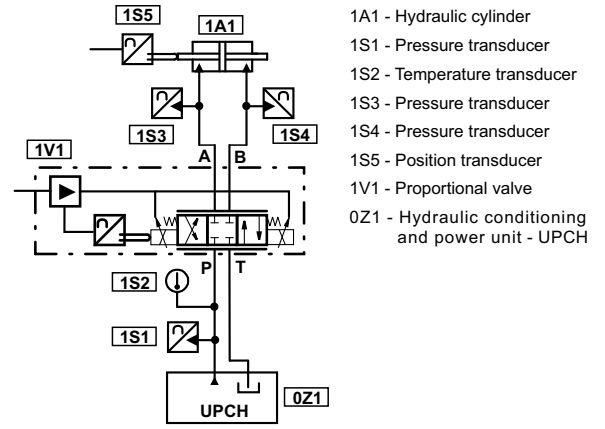
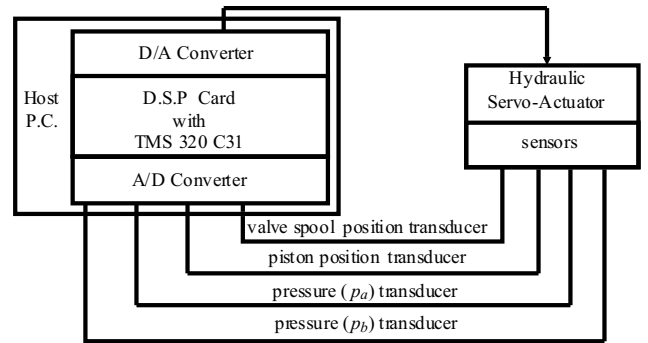


Figure 10. HYDRAULIC CIRCUIT DIAGRAM



- velocity is obtained using a filter and a numeric derivative process

Figure 11. HARDWARE FOR CONTROL SCHEME

In this case, the used dead-zone compensation is given by

$$u_c(u) = \begin{cases} u - c_e & u < -l_c \\ \left( \frac{-c_e + l_c}{l_c} \right) u & -l_c \leq u < 0 \\ \left( \frac{c_d + l_c}{l_c} \right) u & 0 \leq u \leq l_c \\ u + c_d & u > l_c \end{cases} \quad (23)$$

where  $u_c$  is the controller signal. To avoid spool oscillations due to the signal noises, the signal  $u_c$  is smoothed in  $-l_c \leq u \leq l_c$ . The parameters can be identified experimentally [17] and they are:  $c_e = -0.5V$ ,  $c_d = 0.9V$  and  $l_c = 0.05V$ . Figure 12 illustrates this compensation.

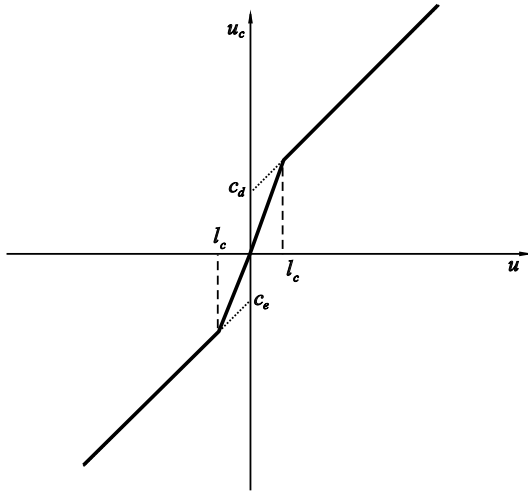


Figure 12. DEAD-ZONE COMPENSATION

## EXPERIMENTAL RESULTS

In this section is presented the experimental results obtained using the cascade controller with the described dead-zone compensation, with and without friction compensation.

The desired position  $y_d(t)$  used in the experiments is presented in Fig. 13 and is given by the time function

$$y_d(t) = \begin{cases} y_{d1}(t) & 0 \leq t < t_i \\ 0.3 & t_i \leq t \leq 2t_i \\ -y_{d1}(t - 2t_i) + 0.3 & 2t_i < t < 3t_i \\ 0 & 3t_i \leq t \leq 4t_i \\ -y_{d1}(t - 4t_i) & 4t_i < t < 5t_i \\ -0.3 & 5t_i \leq t \leq 6t_i \\ y_{d1}(t - 6t_i) - 0.3 & 6t_i < t < 7t_i \\ 0 & 7t_i \leq t \leq 8t_i \end{cases} \quad (24)$$

$$y_{d1}(t) = -2t^7 + 7t^6 - 8.4t^5 + 3.5t^4 \quad (25)$$

where  $t_i = 1s$  is the period in which the actuator is moved according the 7th order polynomial or maintained at rest.

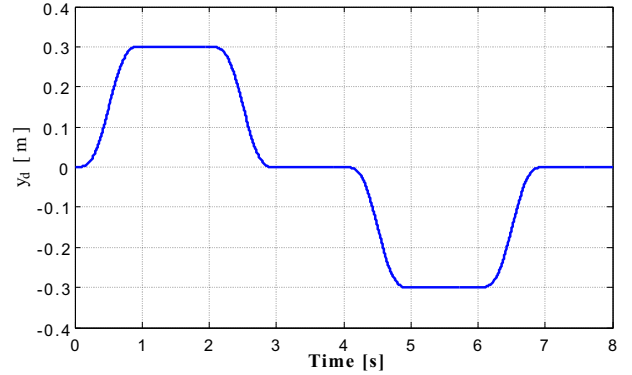


Figure 13. DESIRED POSITION

The cascade controller without friction compensation ( $\hat{F}_A = 0$ ) is referred as CC, and with neural network friction compensation it is referred as CCNN.

The cascade controller gains are tuned according the design rules outlined in [7], and for the adopted sample period of  $t_s = 1 \times 10^{-3}s$  they result in  $K_P = 500s^{-1}$ ,  $\lambda = 25s^{-1}$  and  $K_D = 11000N.s.m^{-1}$ .

The tracking error obtained with the CC controller is shown in Fig.14 and the corresponding control signal is presented in Fig.15. From Fig. 14 is observed that the tracking error converges to a residual set.

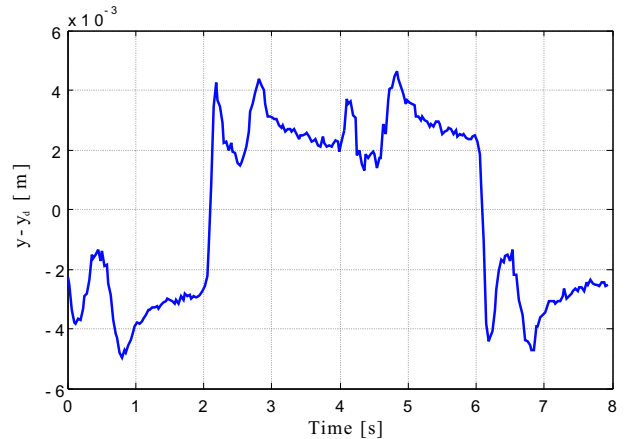


Figure 14. CC CONTROLLER - TRACKING ERROR

Figure 16 presents the tracking error resulting with the CCNN controller and Fig. 17 shows the corresponding control signal. From Fig. 16 is verified that the tracking error converges to a residual set and by comparing with Fig. 14 is concluded that the tracking error using the CCNN controller is smaller than the



tracking error employing the CC controller. This is outlined in Fig. 18, where the two results are compared.

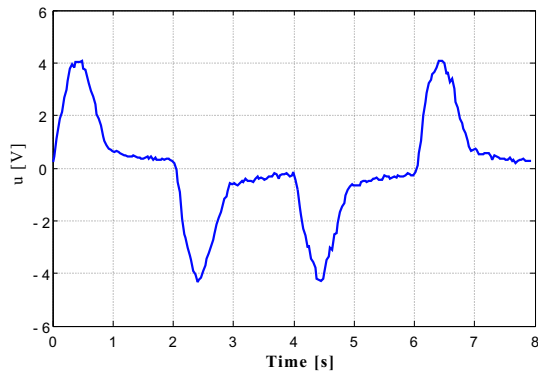


Figure 15. CC CONTROLLER - CONTROL SIGNAL

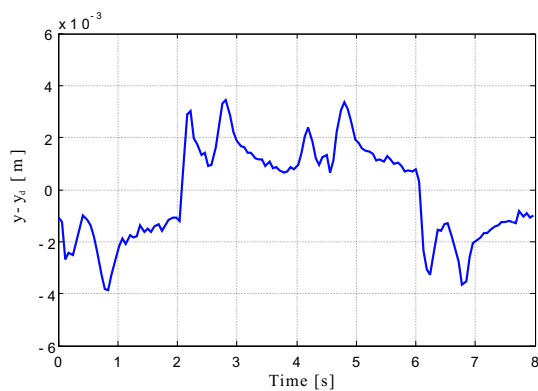


Figure 16. CCNN CONTROLLER - TRACKING ERROR

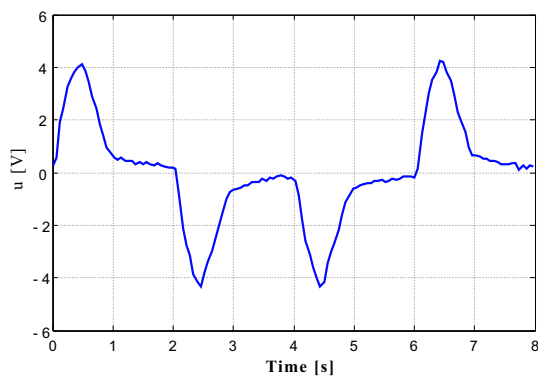


Figure 17. CCNN CONTROLLER - CONTROL SIGNAL

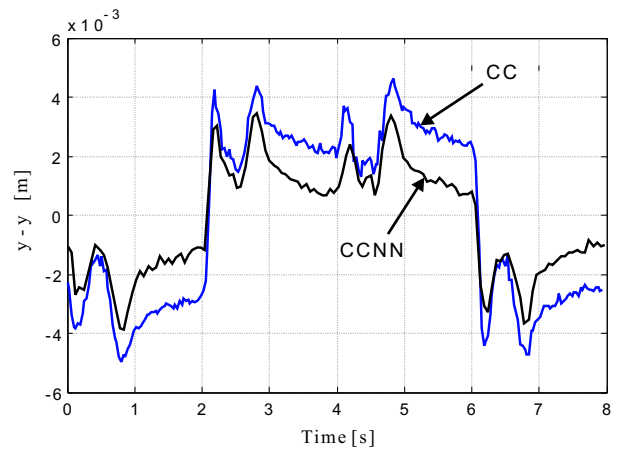


Figure 18. CC AND CCNN - TRACKING ERROR

Despite of the control signals are very similar (see Figs. 15 and 17), the tracking error is smaller using the CCNN because in this case the friction force is partially compensated by the estimated friction force presented in Fig. 19.

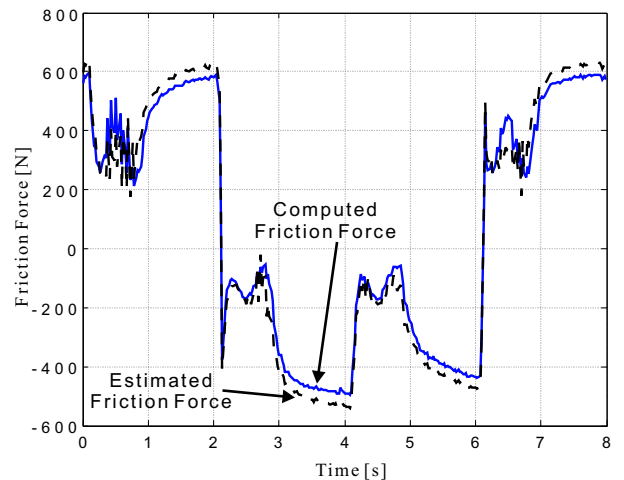


Figure 19. THE ESTIMATED AND COMPUTED FRICTION FORCE

Figure 19 shows the estimated friction force  $\hat{F}_A$  obtained using the trained neural network (Eq. 12) and the computed friction force calculated from Eq. (13). In this figure, it could be observed that the estimated friction force is very near to the computed friction force.

In order to outline the influence of the controller gains in the tracking error, is performed the same experiment using  $\lambda = 30s^{-1}$  instead  $\lambda = 25s^{-1}$ . To this end, is necessary to reduce the sample period to  $t_s = 0.5 \times 10^{-3}s$  as recommended in [7]. The resulting tracking error obtained with the CCNN compared with

the tracking error obtained with CCNN using  $\lambda = 25s^{-1}$  is presented in Fig. 20.

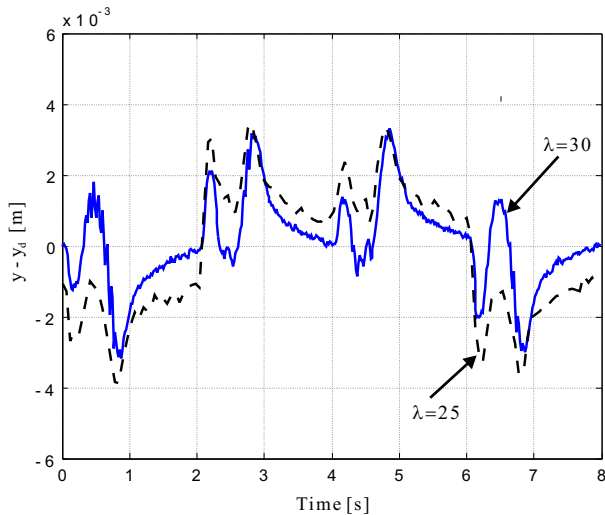


Figure 20. TRACKING ERROR USING  $\lambda = 25s^{-1}$  and  $\lambda = 30s^{-1}$

In Fig. 20, is observed the bettering of the tracking obtained using greater controller gains.

## CONCLUSIONS

In this paper, a neural network to learn the friction force in a hydraulic actuator is proposed to be accomplished with a cascade controller in order to reduce the effects of friction during the tracking of actuators movements.

It is theoretically stated and experimentally confirmed that the tracking error is in fact reduced using the proposed controller. This occurs due to both the good force estimative provided by the neural network and the cascade control characteristics.

The good friction force estimative derives both from the network architecture based on the friction model and the correctness of the training method. The network architecture simplicity, defined after testing several network configurations, has a simple implementation as consequence. By the time, due to its structure, the cascade control technique allows introduce the compensation at the force level on hydraulic actuators.

## ACKNOWLEDGMENTS

This research was partially supported by "Conselho Nacional de Desenvolvimento Científico e Tecnológico (CNPq)", Brazil.

## REFERENCES

[1] Guenther, R., and De Pieri, E. R., 1997. "Cascade control of the hydraulic actuators". *Journal of the Brazilian Society Mechanical Sciences*, **19**(2), pp. 108–120.

[2] Guenther, R., Cunha, M. A. B., De Pieri, E. R., and De Negri, V. J., 2000. "Vs-acc applied to a hydraulic actuator". *Proceedings of American Control Conference*, pp. 4124–4128.

[3] Armstrong-Hélouvry, B., Dupont, P., and Canudas-De-Wit, C., 1994. "A survey of models, analysis tools and compensation methods for the control of machines with friction". *Automatica*, **30**(7), pp. 1083–1138.

[4] Lischinsky, C., Canudas-De-Wit, C., and Morel, G., 1999. "Friction compensation for an industrial hydraulic robot". *IEEE Control Systems Magazine*, **19**, Feb., pp. 25–32.

[5] Sepehri, N., Khayyat, A. A., and Heinrichs, B., 1997. "Cascade control of hydraulically actuated manipulators". *Mechatronics*, **7**(8), pp. 683–700.

[6] Gomes, S. C. P., and Rosa, V., 2003. "A new approach to compensate friction in robotic actuators". *Proceedings of the 2003 IEEE International Conference on Robotics & Automation*, pp. 622–627.

[7] Cunha, M. A. B., Guenther, R., De Pieri, E. R., and De Negri, V. J., 2002. "Design of cascade controllers for a hydraulic actuator". *International Journal of Fluid Power* **3**(2), pp. 35–46.

[8] Bosch Rexroth, 2002. *Proportional control valves*. Bosch Rexroth AG, Industrial Hydraulics, n. 1 987 761 317.

[9] Sepehri, N., Dumont, G. A. M., Lawrence, P. D., and Sassani, 1990. "Cascade control of hydraulically actuated manipulators". *Robotica*, **8**, pp. 207–216.

[10] Heintze, J., Peters, R. M., and Weiden, 1995. "Cascade  $\Delta p$  and sliding mode for hydraulic actuators". *Proceedings of the 3<sup>rd</sup> European Control Conference*, pp. 1471–1477.

[11] Sohl, G. A., and Bobrow, J. E., 1997. "Experiments and simulations on the nonlinear control of a hydraulic servosystem". *Proceedings of American Control Conference*.

[12] Slotine, J., and Li, W., 1988. "Adaptive manipulator control: a case study". *IEEE Transaction on Automatic Control*, pp. 33–44.

[13] Beale, R., and Jackson, T., 1990. *Neural computing: an introduction*. Adam Higler Bristol.

[14] Fausett, L., 1994. *Fundamentals of Neural Networks*. Prentice Hall, New Jersey.

[15] Gervini, V. I., Gomes, S. C. P., and Rosa, V., 2003. "A new robotic drive joint friction compensation mechanism using neural networks". *J. Braz. Soc. Mech. Sci. & Eng.*, **25**(2), pp. 129–139.

[16] Virvalo, T., 1997. "Nonlinear model of analog valve". *5<sup>th</sup> Scandinavian International Conference on Fluid Power*, **3**.

[17] Valdiero, A. C., Guenther, R., and De Negri, V. J., 2005. "New methodology for identification of the dead zone in proportional directional hydraulic valves". *Proceedings of COBEM 2005 – 18<sup>th</sup> International Congress of Mechanical Engineering*.